Tunable AC magnetic hyperthermia efficiency of Ni ferrite nanoparticles

G. Stefanou[a], D. Sakellari[a], K. Simeonidis[a], Th. Kalabaliki[b], M. Angelakeris[a,*], C. Dendrinou-Samara[b] and O. Kalogirou[a]

[a] *Department of Physics, Aristotle University of Thessaloniki, Thessaloniki-54124, Greece*

[b] *Laboratory. of Inorganic Chemistry, Department of Chemistry, Aristotle University of Thessaloniki, Thessaloniki-54124, Greece*

** Corresponding Author: agelaker@auth.gr*

Abstract

Nickel ferrite nanoparticles with sizes lying within the superparamagnetic - ferrimagnetic transition region were synthesized using the solvothermal and the thermal decomposition method. Iron and nickel precursors as well as a variety of surfactants were used at adequate proportions in order to achieve structural and morphological and hence magnetic tuning of the nanoparticles. X-ray diffraction and electron microscopy were used to visualize the actual particle size, morphology and monodispersity aspects and verify the obtained crystal structure. The magnetic hyperthermia response of nickel ferrite nanoparticles and the corresponding mechanisms of heating losses are studied in an effort to unravel the interconnections between the physical properties of magnetic nanoparticles and the tunable AC magnetic hyperthermia efficiency.

Keywords

Magnetic nanoparticles, Magnetic Particle Hyperthermia, Nickel ferrite, Solvothermal, Thermal decomposition.

Introduction

Despite the intensive research of the last decade, the underlying pathogenetic mechanism of cancer development is still far from being fully elucidated due to the fact that many of its risk factors are modifiable over time. Situation might get even more complicated since several factors may act synergistically to induce transformation of normal cells to immortalized cancer ones. The ability of nanotechnology and the corresponding materials to interact with matter at the molecular scale provides not only the possibility to ascertain the molecular signatures of a disease, but also the way they affect the totality of a biological function.[1,2] Magnetic Particle hypethermia (MPH) is a relatively recent complementary anti-cancer therapeutical scheme used in synergy with other techniques such as chemotherapy or irradiation.[34] With this technique, the temperature of a specific region rises, thus cancerous cells undergo a severe thermal shock or are even driven to apoptotic death while healthy cells remain practically unharmed. The driving force is an external AC magnetic field leading the magnetic nanoparticles (MNPs) to produce heat via mechanisms strongly interconnected with their morphological, structural and magnetic profile.[5,6,7] The main energy loss mechanism is relaxation (Néel and/or Brown), if nanoparticles are in the superparamagnetic (SPM) regime,[8] while hysteresis loss mechanism dominates, if MNPs exhibit room temperature ferro(i)magnetism.[9]

Among all systems under research, superparamagnetic iron oxides nanoparticles (SPIONs) have been widely studied in ferrofluid form as multifunctional biomedical agents.[10,11] Since MPH is continuously gaining power as the least invasive cancer treatment, multifunctional heating-triggered modalities initiating from heating response are on the table and the quest of tunable nanomagnetic features pushes the balance from the SPM to ferrimagnetic or even ferromagnetic particles.[12] Following this scheme, it seems sensible to incorporate other ions such as Co^{2+}, Mn^{2+} and Ni^{2+} into typical iron-oxide ferrites, in an effort to attain a diverse spectrum of magnetic features. Within such an approach, ferrite nanoparticles comprise a promising candidate due to their facile fabrication, chemical stability and their inherently relatively low toxicity.[13] Inside the family of the MFe_2O_4 ferrite nanoparticles (where M is usually a divalent ion such as Co^{2+}, Mn^{2+}, Ni^{2+} or Zn^{2+} or a two element combination, such as $Ni_{1-x}Zn_x$), the Ni-based ferrites are generally regarded as highly exploitable materials due to their relatively low cost, high electromagnetic

performance, moderate saturation magnetization, low coercivity and good chemical stability. Despite their soft magnetic features and the mild high frequency degradation, current trends for enhanced performance hyperthermia agents, such systems are still under skepticism for biomedical exploitation.[14,15] The major obstacle of nickel ferrite nanoparticles, is their known cytotoxic effect, i.e., this type of nanoparticles show significantly low viability on HeLa cell at concentrations of 100 μg/mL, while in lower concentration (10 μg/mL) minimal changes on cells proliferation were reported.[16] Moreover, M. Ahamed and co-workers[17] claim that nickel ferrite nanoparticles produce significant cytotoxicity to A549 cells in a dose-dependent manner within the concentration range of 25–100 μg/mL. It should be mentioned here that despite the primitive biocompatibility and toxicity constraints that may hinder eventual implementation, the coverage with the proper coatings may lead to feasible use of such materials in biomedicine.

In the present work, nickel ferrite nanoparticles were synthesized with solvothermal synthesis while reference samples for comparison were also synthesized following a typical thermal decomposition pathway. The solvothermal approach is proposed as a complementary synthetic route providing products of bigger size together with narrow size distributions, limited structural faults, and impurities, also leading to high crystallinity nanoparticles.[18, 19, 20] Furthermore, the role of precursor ratio and surfactant choice (varying molecular weight) was investigated to provide comparative conclusions on chemical stability, reaction yield and reproducibility. The aim of this study is to investigate the amount of heat that nickel ferrite nanoparticles produce in different concentrations when an AC field is applied and how this response may be enhanced. Moreover, the interconnection between the MNPs physical properties, such as size and magnetic characteristics, with the heating efficiency quantified by the Specific Loss Power (SLP) ratio expressed in W/g will be discussed in conjunction with its optimization.[21] It should be mentioned here that despite the actual goal of this work which is to properly tune the soft magnetic Ni-ferrite nanoparticles (morphologically, structurally and magnetically) leading to enhanced heating efficiency compared to SPIONs, toxicity issues should also be successfully addressed in a future work, as in all cases (even for SPIONs with much lower toxicity levels) by a further bio-functionalization step, either by coverage with an organic or inorganic biocompatible layer[22] or by encapsulation in a biocompatible matrix[23] diminishing cytotoxicity effects for living tissues.

Experimental Part

The precursors used in all samples synthesis were $Fe(acac)_3$ and $Ni(acac)_2$ following the methodologies of thermal decomposition and solvothermal synthesis. All chemical reactions were completed in the presence of organic compounds acting as surfactants. The synthetic parameters of all samples under study are summarized in Table I. For the thermal decomposition synthesis (samples T1, T2), a Dewar volatilization was performed to avoid oxidation phenomena. During the process there was a continuous agitation and argon flow to facilitate moisture control and byproducts removal. Finally, by centrifugation and dispersion in the solvent, the MNPs were obtained. The thermal decomposition scheme for Ni based nanoparticles is described in detail in our previous publications.[24,25] For the solvothermal synthesis (samples S1-S4), all reagents were placed in a 20 ml capacity Dewar and then to a 200^{o}C inner temperature oven for 24 hours. After successive washes with low molecular weight solvent and by centrifugation and discarding of the solvent, the final product was obtained. The proposed methodology and parameters of solvothermal synthesis for ferrite nanoparticles (Mn, Ni ferrites) may be sought in our previous works.[26,27] As it can be seen in Table I, polyethylene glycol (PEG) was used in the synthesis (T2, S3, S4) in order to provide directly a biocompatible coverage of the nanoparticles. The best performing MNPs (S2-S4) were eventually redispersed into a biocompatible solvent i.e. dimethyl sulfoxide (DMSO) at three different concentrations (0.5, 1, 2 mg/mL) in an effort to offer an alternative means of nanoparticle stabilization and subsequent fractionation by dispersing the nanoparticles in functional solvents, such as DMSO that serves as both the stabilizing agent and solvent for nanoparticle systems.[27]

Table I: *Methodologies and corresponding synthetic parameters of nickel ferrite MNPs*

Method	Sample	Solvent/Surfactant	Temperature (^{o}C)	Reducing agent
Thermal Decomposition	T1	Oleylamine	200	Hydrazine
	T2	Polyethylene glycol	280	
Solvothermal Synthesis	S1	Benzyl alcohol	200	None
	S2	Benzyl alcohol		
	S3	Polyethylene glycol		
	S4	Polyethylene glycol		

The experimental part included the characterization of nickel ferrite nanoparticles structurally and magnetically by X-ray powder diffraction (XRD), transmission (TEM) and scanning (SEM) electron microscopies and by Vibrating Sample Magnetometry (VSM), respectively, and finally their thermal efficiency evaluation under AC magnetic field.

XRD in conjunction with TEM and SEM were used to identify the Ni-ferrite phases, the particle's morphology, arrangement and size. XRD measurements were performed in a Rigaku Ultima+ powder diffractometer, using Cu(K_α) radiation. TEM observations were carried out in a 100 kV JEM 100CX microscope after depositing drops of the colloidal solutions on carbon-coated copper grids, to verify the obtained crystal structure, the actual particle size and monodispersity. Elemental analysis was carried out by a 20kV JEOL840A SEM equipped with an OXFORD ISIS300 energy dispersive X-ray spectroscopy (EDX) analyzer.An OXFORD Instruments, 1.2 T VSM was used for the magnetic characterization of the nanoparticles. Magnetic loops were recorded at room temperature with maximum field of 800 kA/m, in order to study the dependence of the nanoparticle magnetic characteristics, on their size, structure and stoichiometry. Minor loops were also recorded under 10 and 25 kA/m (minimum and maximum field amplitude of hyperthermia experiments) in order to provide a threshold evaluation of the hysteresis losses as estimated from the DC hysteresis loop area.

Magnetic hyperthermia heating response was measured by subjecting nanoparticles dispersions at different AC magnetic fields generated by an induction heating machine (SPG-10: Ultrahigh Frequency Induction Heating Machine, Shuangping Corporation) of constant frequency 765 kHz and four different AC magnetic field amplitudes (10, 15, 20, 25 kA/m). Despite the use of such a relatively high frequency leading to a rather high $H{\cdot}f$ product[28] (~3×10^{10} $Am^{-1}s^{-1}$>>~ 5×10^{8} $Am^{-1}s^{-1}$ which is the estimated threshold for major discomfort), analogous protocols are currently examined (also in-vitro) as alternatives to overcome the usual constraints of limited heating efficacy.[29,30] All samples were subjected to the AC field for 900 s and then let to cool down, after field removal, for another 900 s. To quantify the heating response, the Specific Loss Power ratio (SLP) was estimated from the heating curves. SLP refers to the energy rate MNPs may provide in their environment when subjected to AC magnetic field and is expressed in W/g. SLP has to be maximized in accordance to MNPs properties and applied field parameters. In general, the initial temperature rising slope was found to be proportional to the magnitude of applied magnetic field and concentration and

was used as the experimental input in the SLP calculation incorporating also data correction to avoid SLP overestimations due to non magnetic heating contributions.[31,32]

Results and Discussion

In Figure 1, the XRD patterns for all samples under study are given. Samples were identified to crystallize in the cubic Ni–ferrite phase. The major peak of the XRD spectrum corresponds to the (311) reflection of nickel ferrite in all cases, appearing at 35.5 degrees (2θ). In all samples several sharp peaks are being displayed, which lead to the conclusion that the nanoparticles are highly crystallized. Furthermore, the full width at half maximum (FWHM) diminishes as the MNP size raises. In general, using the solvothermal synthesis, the XRD patterns present sharper and narrower peaks, indicating not only larger MNPs but a highly crystalline structure as well. The mean size of nickel ferrite nanoparticles as calculated using the Scherrer's formula appears at Table II. The cubic lattice parameters were calculated to vary from a = 8.302 Å (T1) to a = 8.365 Å (S4), respectively, in the region of the bulk $NiFe_2O_4$ (a = 8.337 Å), in agreement with previous reports on analogous sizes of MNPs.[27] Figure 1 also contains two representative TEM images: T2 sample for thermal decomposition and S2 sample for solvothermal synthesis. TEM observations revealed the spherical shape of nanoparticles and their self-assembly arrangements indicating the successful role of the surfactants incorporated. From series of low magnification (similar to the ones shown in Fig.1) TEM images for each sample, the mean particle size was estimated based on 200 MNPs in each case and the corresponding histograms were successfully fitted with standard lognormal distribution functions, also collected in Table II, showing good agreement with the XRD crystallite estimations. As shown in Table II, Ni/Fe precursor ratio was an adjustable parameter affecting nanoparticle stoichiometry and average nanoparticle size. In principle, the thermal decomposition samples exhibit narrow size distributions, while samples prepared by solvothermal synthesis generally show broader size distributions. Here, it seems that by the proper choice of surfactants acting potentially as solvents and reducing agents such issues may be satisfactorily addressed and the solvothermal approach may be reintroduced.[19,20,27] Since the reaction conditions are easily reproducible and can be further scaled up for massive production, the solvothermal synthetic route seems more appropriate for bigger average-size MNPs covered with adequate biocompatible surfactants.[19]

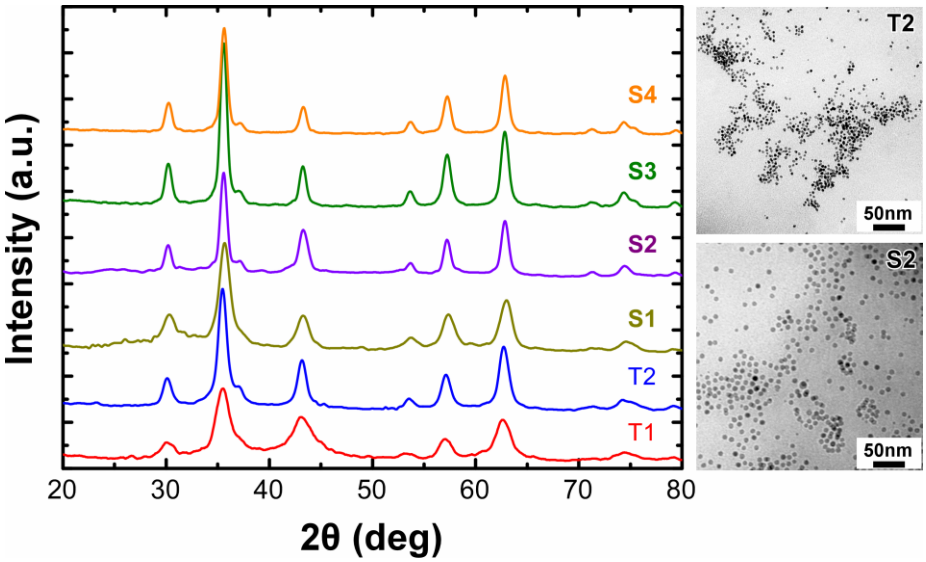

Figure 1: *left: X-ray diffraction patterns for samples under study; right: TEM imaging for two representative cases; top image: sample T2 prepared by thermal decomposition; bottom image: sample S2 prepared by solvothermal synthesis.*

Table II: *Structural and magnetic features of nickel ferrite MNPs under study*

Sample	Ni/Fe molar ratio (synthesis)	Ni/Fe atomic ratio (EDX)	XRD Size (nm)	TEM Size (nm±10%)	M_s (A m^2/kg)	H_c (kA/m)	M_r (A m^2/kg)
T1	1 : 1	1.0/2.0	4.2	4.0	22.3	5.0	1.0
T2	2 : 1	1.2/1.8	5.3	5.0	36.3	5.5	4.7
S1	3 : 1	1.2/1.8	6.2	6.0	27.3	3.8	1.5
S2	2 : 1	1.0/2.0	7.8	8.0	43.9	11.0	10.4
S3	1 : 1	0.8/2.2	13.0	14.0	55.9	9.0	21.4
S4	1 : 2	0.6/2.4	15.8	16.0	68.6	7.0	16.4

Nickel ferrites are typical ferrimagnetic materials. They constitute of two oppositely directed magnetic sublattices and exhibit collective magnetic features such as hysteresis and magnetic saturation.[33] Hysteresis loops were recorded at room temperature by VSM. The saturation magnetization (M_s), magnetic remanence (M_r) and coercivity (H_c) measured for all samples were found to be strongly dependent on the mean nanoparticle size (see Table II) as it depicted in Figure 2 for M_s. Blue diamonds refer to MNPs synthesized with thermal decomposition and red circles to those synthesized with solvothermal synthesis. It can be observed that saturation magnetization varied from ~22 up to ~70 Am^2/kg, showing a linear dependence with the size irrespective of the synthesis method surpassing occasionally as

discussed later on bulk nickel ferrite magnetization value. Magnetic remanence, up to 21 Am^2/kg, adopts a similar trend as it increases in proportion to the nanoparticle size.

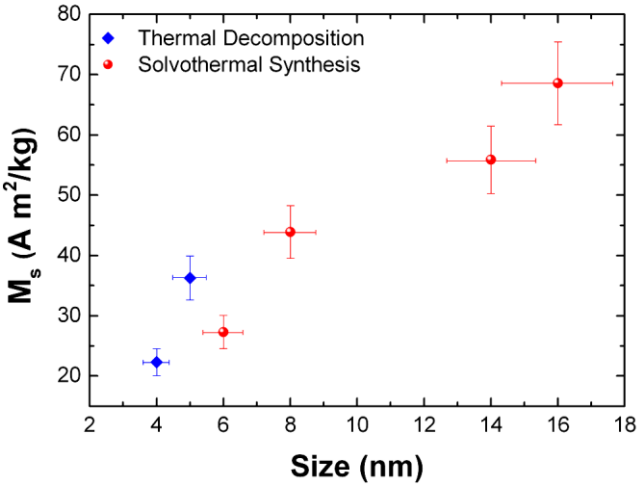

Figure 2: *Dependence of saturation magnetization of Ni-ferrite MNPs on their average size.*

Nickel ferrite nanoparticles possess the inverse spinel structure, under the formula $(Fe^{3+})_A(Ni^{2+}Fe^{3+})_B O_2^{2-}$, where A denotes tetrahedral and B octahedral sites. Nickel has the tendency to occupy octahedral sites while iron tetrahedral ones.[34] In the case of the stoichiometric Ni ferrites, in each unit cell only eight iron ions occupy the A sites and the remaining eight fill the B sites along with Ni ions yielding a net magnetization value of 55 Am^2/kg for the bulk stoichiometric Ni ferrite.[35] The net magnetization arises from the antiparallel sublattice magnetizations, $M=M_B-M_A$, hence, it is affected by the occupancy of two different sublattices by Ni/Fe ions. When in the cubic cell, Ni is deficient and iron is over-stoichiometric, as mostly in our samples (3rd column of Table II), apart from the eight in A-site and the eight in B-site iron ions that cancel each other, the ions that will sum up to give the net magnetization comprise of the nickel and remaining iron ions. Furthermore, taking in mind that magnetic moment of Fe^{3+} is bigger ($5\mu_B$) than Ni^{2+} ($2\mu_B$), one can conclude that the net magnetization for nickel deficient ferrites may grow even bigger than the bulk value of stoichiometric nickel ferrite. Contrary, the nanosized dimensions of the MNPs have a negative effect on net magnetization,[13] thus this controversy favors enhanced magnetization only for the bigger MNPs of S4.

On the first stage of the AC magnetic hyperthermia experimental procedure, all samples had their heating efficiency tested under four different field amplitudes and over the same concentration of 1 mg/mL in the as prepared colloidal form. To adequately address

the magnetic particle hyperthermia issue, MNPs colloids should at least lead to a temperature rise more than 4°C, where a much larger rise guarantees their efficiency also in subsequent in-vitro and in-vivo stages where due to immobilization of MNPs within cells SLP records are hindered.[36]

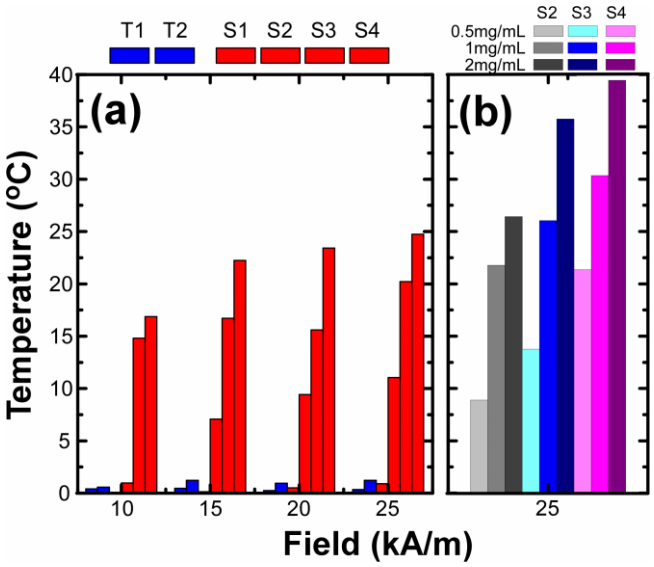

Figure 3: *Temperature rise of ferrite nanoparticles at (a) concentration of 1 mg/mL and all magnetic field intensities and (b) at three different concentrations after redispersion in biocompatible DMSO medium and under the strongest magnetic field, the color of each triplet of concentrations gets darker as the sample gets denser. The bars follow the sequence of the line that appears at the top of each figure.*

Figure 3a depicts the temperature rise after subtracting the reference signal due to the solvent for all field intensities and for the concentration of 1 mg/mL. Blue colored bars stand for samples prepared by thermal decomposition (T1, T2) and red colored bars (S1-S4), for solvothermal synthesis appearing in sequential order. It is obvious, that the larger the field amplitude, the higher the temperature levels exhibited by the MNPs regardless from the synthesis method. In general, the group of MNPs with the better performance was the solvothermal one, particularly samples S2, S3, S4. This trend is readily connected with size regimes presented in Table II. Heating efficiency increases significantly, when particle size grows beyond 7 nm where MNPs yield a more rigid ferrimagnetic attitude (as described by the combinatory increase of M_s, H_c and M_r) also discussed in our previous works.[12,21,32] For instance T2, though possessing a relatively high saturation magnetization, it exhibits a negligible temperature rise due to its rather small H_c and M_r. On the contrary, best performing particles (S2, S3, S4) exhibiting significant temperature increases of ~25°C (at 25 kA/m, 1 mg/mL) possess stronger ferrimagnetic features that seem directly exploitable for magnetic particle hyperthermia.

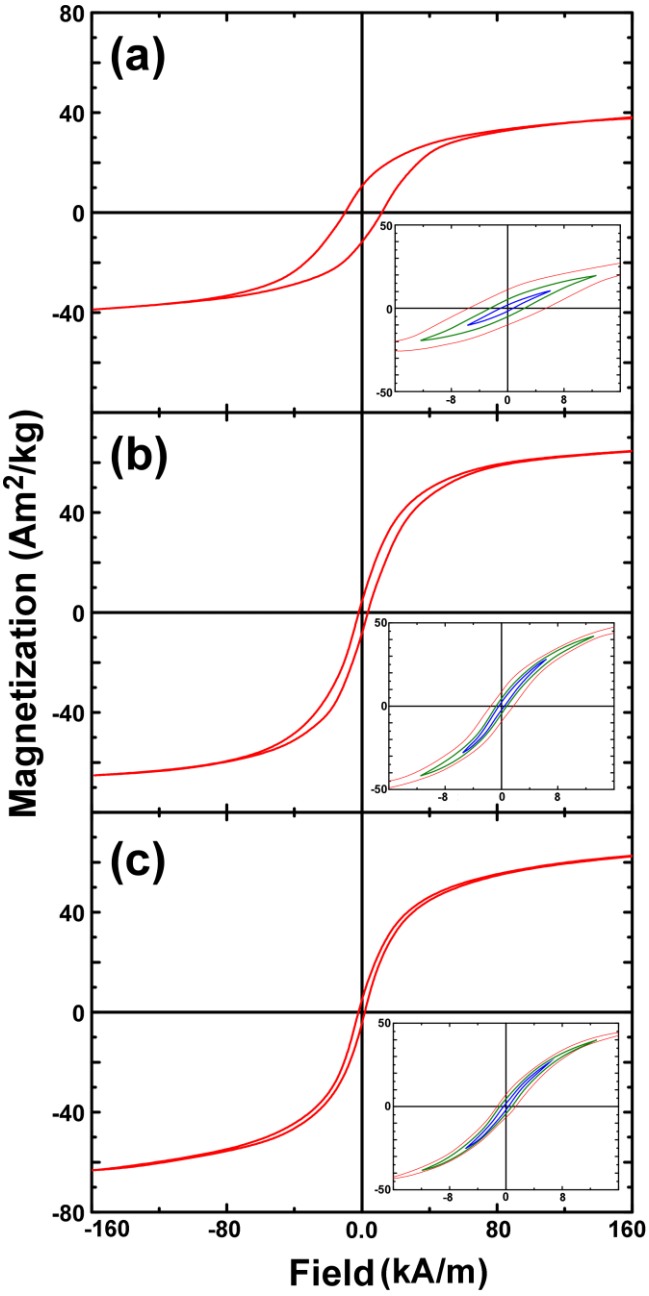

Figure 4: *Room temperature full hysteresis (outside curve in red color) of (a) S2, (b) S3 and (c) S4. Lower right insets are magnification of hysteresis loop central parts together with corresponding minor loops at the applied AC hyperthermia magnetic field amplitudes (inner loop(blue): 10 kA/m, outer loop(green): 25 kA/m).*

On a second stage, the three best performing samples (S2, S3, S4) were redispersed in the biocompatible solvent DMSO and undergone hyperthermia experiments under the same magnetic fields in three different concentrations 0.5, 1 and 2 mg/mL (Figure 3b) in an effort to examine the stability of optimized heating response. The slight improvement of temperature rise of 1 mg/mL MNPs when dispersed in DMSO solvent may be correlated with increased colloidal stability.[27,37] This second set of measurements supplements the

temperature dependence of concentration showing temperature rise up to 40^{o}C, again following the size increase of the particles.

The major characteristic that discriminates MNPs suitable for heat-triggered biomedical applications, is the amount of heat (energy) they produce, when subjected to alternate magnetic field. The energy loss is described by the SLP that should be maximized in order to have the minimum dose applied, to eliminate as much as possible potential side-effects. The fact that samples S2, S3 and S4 exhibit typical ferrimagnetic behavior at room temperature, strengthens their potential as hyperthermia agents since larger hysteresis loops generally result to higher AC magnetic hysteresis losses. In Figure 4, characteristic hysteresis loops are shown for three samples (S2, S3 and S4) recorded at 300 K under maximum applied field of 800 kA/m showing measurable coercive field and approach to saturation at room temperature. The slight decrease of coercive field (values appear in Table II) as particle size increases may be attributed to the monodomain to multidomain transition directly connected with coercivity attenuation. In order to have a theoretical estimation of the heating efficiency via hysteresis losses VSM loops at fields up to 10 and 25 kA/m (the same as in hyperthermia measurements) were also recorded, separated by individual demagnetizing cycles (insets in Figure 4). Although the static magnetic behavior as recorded by VSM magnetometry is distinctively different from the dynamic AC response during hyperthermia cycles, the minor loop loss estimation are only serving as a threshold-guideline of the hysteresis losses heating efficiency. The field and concentration dependence of SLP are shown in Figures 5a and 5b respectively. In all cases as the magnetic field increases, the SLP follows. In Figure 5b, for all samples an SLP drop with concentration is exhibited. In all cases, SLP values remain at relatively high levels (>120 W/g) with the bigger in size particles approaching 400 W/g. Our SLP records for Ni-ferrite sample compare relatively well not only with relevant studies in ferrite[13] but with iron-oxide samples[37] as well showing the potential of such systems as hyperthermia carriers if properly tuned.[38] It is apparent that the harder the magnetic features the better the heating efficiency. The differences in SLP values among the three samples are directly connected with their sizes and corresponding magnetic features (as shown in Table II). Moreover, as concentration increases dipolar interactions among the MNPs may also increase and the AC hyperthermia magnetic field encounters more obstacles in manipulating MNPs, thus smaller SLP values appear. A model explaining the concentration behavior of SLP has been proposed by some of us in the work of C.

Martinez-Boubeta et al.[12] where it is proposed that when the particles are situated far apart from each other (low concentrations) they do not interact so the SLP increases with concentration basically due to individual intrinsic MNPs features. For bigger concentrations, the magnetic interactions increase leading to MNP aggregates and thus SLP drops, since magnetic interaction competes with the external field.

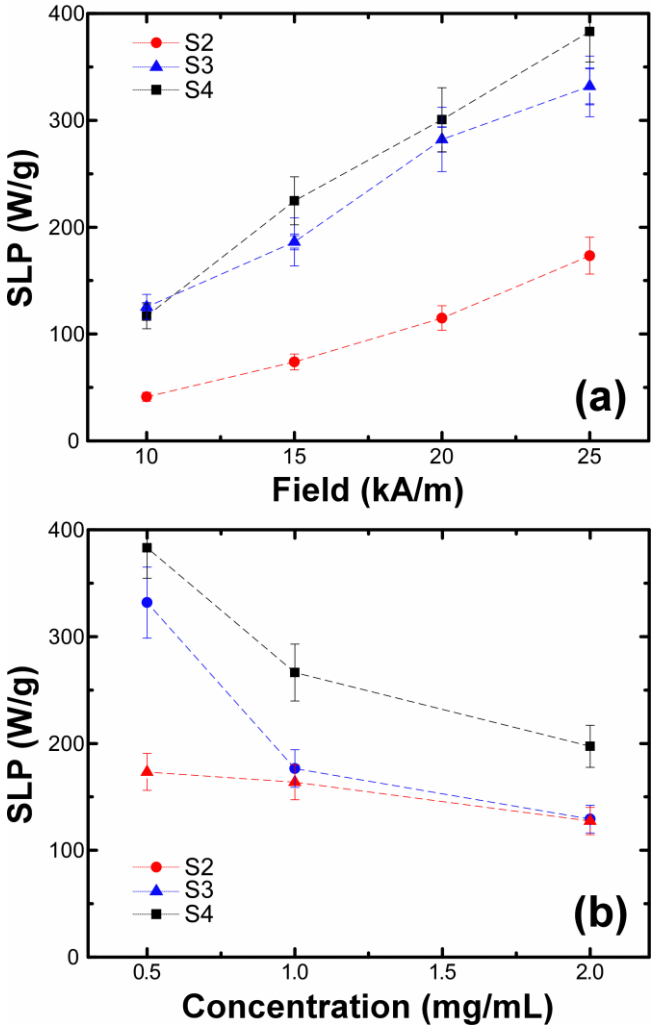

Figure 5: *Specific Loss Power (SLP) effects: (a) field dependence at the smallest solution concentration of the 0.5mg/mL (b) concentration dependence of SLP at higher field amplitude of 25 kA/m.*

The heat produced by nanoparticles and quantified by the SLP factor, derives from different mechanisms, i.e., eddy currents, Néel (τ_N) and Brown (τ_B) relaxation, and hysteresis losses. The nanoparticles' size (4-16 nm) safely exclude eddy currents mechanism as negligible,[13] thus reducing the number of energy loss mechanisms mainly to magnetic-origin ones. Since samples S2-S4 are in ferrimagnetic state at room temperature, the predominant losses mechanism may be attributed to hysteresis losses.[21] In order to have a qualitative

estimation, we have calculated hysteresis losses from the corresponding hysteresis minor loops areas (insets in Figure 4). Estimated values are 189, 306 and 326 W/g for samples S2, S3 and S4 respectively at maximum field amplitude of 25 kA/m. As discussed previously, these values since they are calculated via a quasi-static magnetic measurement are underestimated, yet they show that hysteresis losses dominate over SLP, in good agreement to relevant studies in ferrite nanoparticles.[39, 40] Eventually, Ni-ferrite magnetic nanoparticles yielding tunable ferrimagnetic features comprise a promising candidate for further exploration as hyperthermia carriers, provided colloidal stabilization and biocompatibility ability are satisfactorily addressed in the upcoming in vitro and in vivo experiments.

CONCLUSIONS

In this work nickel ferrite particles were synthesized in an effort to tune their structural and morphological features towards enhanced AC heating mediators. Spherical particles of 4-16 nm in size were synthesized, characterized by XRD, TEM and VSM and found to be Ni-ferrites with size-tunable magnetic features. The AC heating response of these particles arises mainly from the ferrimagnetism shown at room temperature and sets these systems as promising candidates for Magnetic Particle Hyperthermia provided the cytotoxicity issues are safely resolved by proper surfactant coatings. Larger size particles (> 10 nm) possess significant SLP values that can be further optimized under different field conditions, colloidal choice and particle properties.

REFERENCES

1 World Health Organization: www.who.int/cancer/prevention/en/

2 C.S.S.R. Kumar, F. Mohammad, “Magnetic nanomaterials for hyperthermia-based therapy and controlled drug delivery”, *Advanced Drug Delivery Reviews,* vol. 63, p. 789, 2011.

3 M.B. Lopez, “Magnetic nanoparticle-based hyperthermia for cancer treatment”, *Reports of practical oncology and radiotherapy,* vol. 1, Iss. 8, p. 397, 2013.

4 I. Hilger, “In vivo applications of magnetic nanoparticle hyperthermia”, *Int. J. Hyperthermia*, vol. 29(8), pp. 828–834, 2013.

5 R. Hergt, S. Dutz, R. Muller and M. Zeisberger, “Magnetic particle hyperthermia: nanoparticle magnetism and materials development for cancer therapy”, *J. Phys.: Condens. Matter*, vol. 18, pp. 2919–2934, 2006.

6 G. Salas, S. Veintemillas-Verdaguer, M. del Puerto Morales, “Relationship between physico-chemical properties of magnetic fluids and their heating capacity”, *Int. J Hyperthermia*, vol. 29(8), pp. 768–776, 2013.

[7] S. Dutz, R. Hergt, Magnetic nanoparticle heating and heat transfer on a microscale: Basic principles, realities and physical limitations of hyperthermia for tumour therapy, *Int. J. Hyperthermia*, vol. 29(8), pp. 790–800 2013.

[8] R. E. Rosensweig, "Heating magnetic fluid with alternating magnetic field", *J. Magn. Magn. Mater.* vol. 252, pp. 370–374, 2002.

[9] E. Kita, T. Oda, T. Kayano, S. Sato, M. Minagawa, H. Yanagihara, M. Kishimoto, C. Mitsumata, S. Hashimoto, K. Yamada, N. Ohkohchi, "Ferromagnetic nanoparticles for magnetic hyperthermia and thermoablation therapy", *J. Phys. D: Appl. Phys.*, vol. 43, p. 474011, 2010.

[10] L.H. Reddy, J. L. Arias, J. Nicolas and P. Couvreur, "Magnetic Nanoparticles: Design and Characterization, Toxicity and Biocompatibility, Pharmaceutical and Biomedical Applications", *Chem. Rev.*, vol. 112, pp. 5818−5878, 2012.

[11] S. Laurent, S. Dutz, U. O. Häfeli, M. Mahmoudi, "Magnetic fluid hyperthermia: Focus on superparamagnetic iron oxide nanoparticles", *Advances in Colloid and Interface Science* vol. 166 [1–2] 10, pp. 8–23, 2011.

[12] C. Martinez-Boubeta, K. Simeonidis, David Serantes, I. Conde-Leborán, I. Kazakis, G. Stefanou, L. Peňa, R. Galceran, Ll. Balcells, C. Monty, D. Baldomir, M. Mitrakas, and M. Angelakeris, "Adjustable Hyperthermia Response of Self-Assembled Ferromagnetic Fe-MgO Core–Shell Nanoparticles by Tuning Dipole–Dipole Interactions", *Adv. Func. Mater.* vol. 22, Iss. 17, pp. 3737–3744, 2012.

[13] I. Sharifi, H. Shokrollahi, S. Amiri, "Ferrite-based magnetic nanofluids used in hyperthermia applications", *J. Magn. Magn. Mater.* vol. 324, pp. 903–915, 2012.

[14] E.L. Verde, G. T. Landi, M. S. Carrião, A. L. Drummond, J. A. Gomes, E. D. Vieira, M. H. Sousa, and A. F. Bakuzis, "Field dependent transition to the non-linear regime in magnetic hyperthermia experiments: Comparison between maghemite, copper, zinc, nickel and cobalt ferrite nanoparticles of similar sizes", *AIP Advances*, vol. 2, p. 032120, 2012.

[15] A. Tomitaka, H. Kobayashi, T. Yamada, M. Jeun, S. Bae, and Y. Takemura, "Magnetization and self-heating temperature of $NiFe_2O_4$ nanoparticles measured by applying ac magnetic field", *J. Phys.: Conf. Ser.* vol. 200 p. 122010, 2010.

[16] A. Tomitaka, A. Hirukawa, T. Yamada, S. Morishita, and Y. Takemura, "Biocompatibility of various ferrite nanoparticles evaluated by in vitro cytotoxicity assays using HeLa cells", *J. Magn. Magn. Mater.*, vol. 321, pp. 1482–1484, 2009.

[17] M. Ahamed, M. J. Akhtar, M. A. Siddiqui, J. Ahmad, J. Musarrat, A. A. Al-Khedhairy, M. S. Al-Salhi, S. A. Alrokayan, "Oxidative stress mediated apoptosis induced by nickel ferrite nanoparticles in cultured A549 cells", *Toxicology* vol. 283, pp. 101–108, 2011.

[18] S. Guo, D. Li, L. Zhang, J. Li, E. Wang, "Monodisperse mesoporous superparamagnetic single-crystal magnetite nanoparticles for drug delivery", *Biomaterials*, vol. 30, pp. 1881–1889, 2009.

[19] G. Demazeau, "Solvothermal processes: new trends in materials chemistry", *J. Phys.: Conf. Ser.* vol. 121, p. 082003, 2008.

[20] G. Demazeau, "Impact of high pressures in solvothermal processes", *J. Phys.: Conf. Ser.* vol. 215, p. 012124, 2010.

[21] K. D. Bakoglidis, K. Simeonidis, D. Sakellari, G. Stefanou, M. Angelakeris, "Size-Dependent Mechanisms in AC Magnetic Hyperthermia Response of Iron-Oxide Nanoparticles", *IEEE Trans. Magn.* vol. 48 4, pp. 1320-1323, 2012.

[22] T.D. Schladt, K. Schneider, H. Schild, and W. Tremel, "Synthesis and bio-functionalization of magnetic nanoparticles for medical diagnosis and treatment", *Dalton Transactions,* vol. 40, p.6315, 2011.

[23] M. Filippousi, T. Altantzis, G. Stefanou, M. Betsiou, D. N. Bikiaris, M. Angelakeris, E. Pavlidou, D. Zamboulis and G. Van Tendeloo, "Polyhedral iron oxide core–shell nanoparticles in a biodegradable polymeric matrix: preparation, characterization and application in magnetic particle hyperthermia and drug delivery", *RSC Adv.* vol. 3, p. 24367, 2013.

[24] S. Mourdikoudis, K. Simeonidis, A. Vilalta-Clemente, F. Tuna, I. Tsiaoussis, M. Angelakeris, C. Dendrinou-Samara and O. Kalogirou, "Controlling the crystal structure of Ni nanoparticles by the use of alkylamines", *J. Magn. Magn. Mater.* vol. 321 pp. 2723–2728, 2009.

[25] A. Kotoulas, M. Gjoka, K. Simeonidis, I. Tsiaoussis, M. Angelakeris, O. Kalogirou, C. Dendrinou-Samara, "The role of synthetic parameters in the magnetic behavior of relative large hcp Ni nanoparticles", *J. Nanopart. Res.* vol. 13, pp.1897-1908, 2011.

[26] K. Vamvakidis, D. Sakellari, M. Angelakeris, C. Dendrinou-Samara, "Size and compositionally controlled manganese ferrite nanoparticles with enhanced magnetization", *J. Nanopart. Res.* vol. 15, p. 1743, 2013.

[27] M. Menelaou, K. Georgoula, K. Simeonidis and C. Dendrinou-Samara, "Evaluation of nickel ferrite nanoparticles coated with oleylamine by NMR relaxation measurements and magnetic hyperthermia", *Dalton Transactions*, vol. 43(9), pp. 3626-36, 2014.

[28] S.E. Barry, Int. J. Hyperthermia, "Challenges in the development of magnetic particles for therapeutic applications", vol. 24, pp. 451–466, 2008.

[29] Q.A. Pankhurst, N.K.T. Thanh, S.K. Jones and J. Dobson, "Progress in applications of magnetic nanoparticles in biomedicine", *J. Phys. D: Appl. Phys*, vol. 42, p. 224001, 2009.

[30] B. Kozissnik, A. C. Bohorquez, J. Dosbon, C. Rinaldi, "Magnetic fluid hyperthermia: Advances, challenges, and opportunity", *Int. J. Hyperthermia*, vol. 29(8)**,** pp. 706-14, 2013.

[31] A. Chalkidou, K. Simeonidis , M. Angelakeris, T. Samaras, C. Martinez-Boubeta, Ll. Balcells, K. Papazisis, C. Dendrinou-Samara, O. Kalogirou, "In vitro application of Fe/MgO nanoparticles as magnetically mediated hyperthermia agents for cancer treatment", *J. Magn. Magn. Mater.* vol. 323, pp. 775–780, 2011.

[32] K. Simeonidis, C. Martinez-Boubeta, Ll. Balcells, C. Monty, G. Stavropoulos, M. Mitrakas, A. Matsakidou, G. Vourlias, M. Angelakeris, "Fe-based nanoparticles as tunable magnetic particle hyperthermia agents", *J. Appl.Phys.* vol. 114, p. 103904, 2013.

[33] A.H. Morrish, "The Physical Principles of Magnetism", *IEEE Press Classic Reissue*, 2001.

[34] J. Smit, H.P.J. Wijn, "Ferrites—Physical Properties of Ferromagnetic Oxides in Relation to their technical Applications", *John Wiley and Sons*, New York 1959.

[35] A. Goldman, *Modern Ferrite Technology*, 2nd edition, Sp.57, Springer 2006.

[36] G. Glöckl, R. Hergt, M. Zeisberger, S. Dutz, S. Nagel and W. Weitschies, "The effect of field parameters, nanoparticle properties and immobilization on the specific heating power in magnetic particle hyperthermia", *J. Phys.: Condens. Matter* vol. 18, pp. S2935–S2949, 2006.

[37] C. Grüttner, K. Müller, J. Teller, F. Westphal, "Synthesis and functionalisation of magnetic nanoparticles for hyperthermia applications", *Int. J. Hyperthermia*, vol. 29(8), pp. 777–789, 2013.

[38] G. Bellizzi and O. M. Bucci, "On the optimal choice of the exposure conditions and the nanoparticle features in magnetic nanoparticle hyperthermia", *Int. J. Hyperthermia*, vol. 26 (4), p. 389, 2010.

[39] M. Jeun, S. Bae, A. Tomitaka, Y. Takemura, K. H. Park, S. H. Paek, K.-W. Chung, "Effects of particle dipole interaction on the ac magnetically induced heating characteristics of ferrite nanoparticles for hyperthermia", *Appl. Phys. Lett.* vol. 95, p. 082501, 2006.

[40] O.V. Yelenich, S. O. Solopan, T. V. Kolodiazhnyi , V. V. Dzyublyuk, A. I. Tovstolytkin, A. G. Belous, “Superparamagnetic behavior and AC-losses in $NiFe_2O_4$ nanoparticles”, *Solid State Sciences*, vol. 20, pp. 115-119, 2013.